Lancaster University

Industrial Group Project Report
Create An 'All-In-One' Control For Fatigue Crack Growth Rate Testing

Dominic Jack Reeves

Degree Scheme: MPhys Hons Physics

Module: Phys355 - Industrial Group Project

Year of Study: Third Year

March 23, 2017

Abstract

This report covers the design and creation of a prototype for a fatigue crack growth rate system. This system both controls the hardware components of the system and analyses all the returning data into a form that holds meaningful physical value for determining the fatigue toughness of a system. The outcome of the project was a prototype with sufficient functionality to control and analyse the main factors involved in fatigue crack growth rate testing with errors in the analysis calculations, compared to the currently implemented system, of no higher than a 0.01 fractional difference. The main factors analysed in this system were the crack size, crack growth rate and stress intensity factor; all of which are used to estimate the number of cycles of stress a material can withstand before the crack evolution rate grows too high.

Contents

1 Introduction

This report covers the design / creation of an all-in-one control system for a fatigue crack growth rate (from here on referred to as FCGR) system as well as the error testing of the system. This is the project that was brought to the group by our industrial contact Matthew Thomas representing the firm Exova. The fatigue crack growth rate of a material indicates how a crack in a material is going to propagate with time while under a cyclic stress. [4]. As such, FCGR testing is used as a measure of material toughness in the automotive, aerospace and power generation sectors [2] and is normally given in the form of change in crack length per cycle $\frac{da}{dn}$ against stress intensity factor range ΔK. For our project we were to adhere to two sets of standards and calculations, the British Test Standards (BS ISO) [3] and American Section of the International Association for Testing Materials (ASTM) [1].

1.1 Briefing

The briefing we were given stated that we were to 'Design and manufacture a system that will control a test frame and capture the required raw test data to measure fatigue crack growth rates in coupon test pieces via the direct current potential drop and clip gauge compliance methods. The system shall be capable of various loading regimes and waveforms. The system must meet the requirement of various international testing standards.' Specifically they asked for:

- All testing is to be conducted in accordance with ASTM E647 [1], BS ISO 12108 [3].
- The system needs to be stand-alone (current pulse, waveform generation, data recording).
- The current required for generating an acceptable voltage response can be in excess of 30A.
- The waveform can be supplied to the test frame via a scaled ± 10 output generated by the system and delivered via a coaxial cable fitted with a BNC connector. Feedback from the load channel will be returned from the test rig controller in a similar manner.
- Current shall be generated by the system and delivered to the sample with the voltage response measured and recorded from the test piece and the reference piece by the system.
- All test data is to be recorded by the system.
- The system should be capable of performing the following types of FCGR testing:
  - Increasing K (constant load).
  - Constant K (load sheading).
  - Decreasing K or Threshold (load sheading)
- Utilising the following waveforms:
  - Sinusoidal
  - Sinusoidal Overload
  - Triangular
  - Trapezoidal
  - Trapezoidal Overload
  - Spectrum

- For the following sample geometries:
  - Compact Tension (CT)
  - Single edged notch bend (SE(8))
  - Corner Cracked (CC)
  - Semi-elliptical (Kb or Kbr)
- System Requirements
  - The system should be capable of terminating the test on the following criteria
    * Cycles
    * Crack Length
    * Relative Voltage Change
    * Absolute Voltage Change
    * Suspect set-up (loss of circuit continuity)
    * Loss of control / mean or amplitude error
    * Specimen failure
  - The system needs to be capable of capturing the following data:
    * Peak-Valley loads
    * Current-on values (test piece and reference piece)
    * Current-off values (test piece and reference piece)
    * 2 temperature channels
  - Data needs to be accessible while the test is running

1.2 Motivations

The current system that Exova Lancaster runs is provided by a third party supplier and each licensed copy of the program comes with an associated cost. As a result of this, Exova are interested in developing their own in-site system, both for the additional adaptiveness as well as the reduction in cost. As a result of this they asked us to produce a prototype of the above described system as a proof of concept for one of the systems that they would like to develop their own version of.

2 Theory

To measure the FCGR toughness a notched specimen with a pre-existing crack is put under a cyclic fatigue loading. It is important that the stress due to load applied is predominantly within the materials elastic range [3].The change in crack length with respect to the change in cycles, $\frac{da}{dn}$ in terms of the crack tip stress intensity range ΔK can be used as a measurement of the toughness [1] and compared to various international testing standards; in this case the ASTM E647, BS ISO 12108 and customer requirements.

2.1 The Process of Fatigue Crack Growth Rate

FCGR testing, as described by the American [1] and British [3] standards will be outlined in this section. FCGR testing starts with the pre-cracking stage by machining a notch (or crack) into the material in a given geometry, this notch can, from then on, be seen as the origin of any crack evolved during the testing process. The material sample is then loaded into the test frame via pins machined in to each side and a cyclic load is applied to the material, with a cycle being defined as the time taken for the force to vary from one peak to the next. An example of a machined notch in the CT geometry can be seen in figure 1.

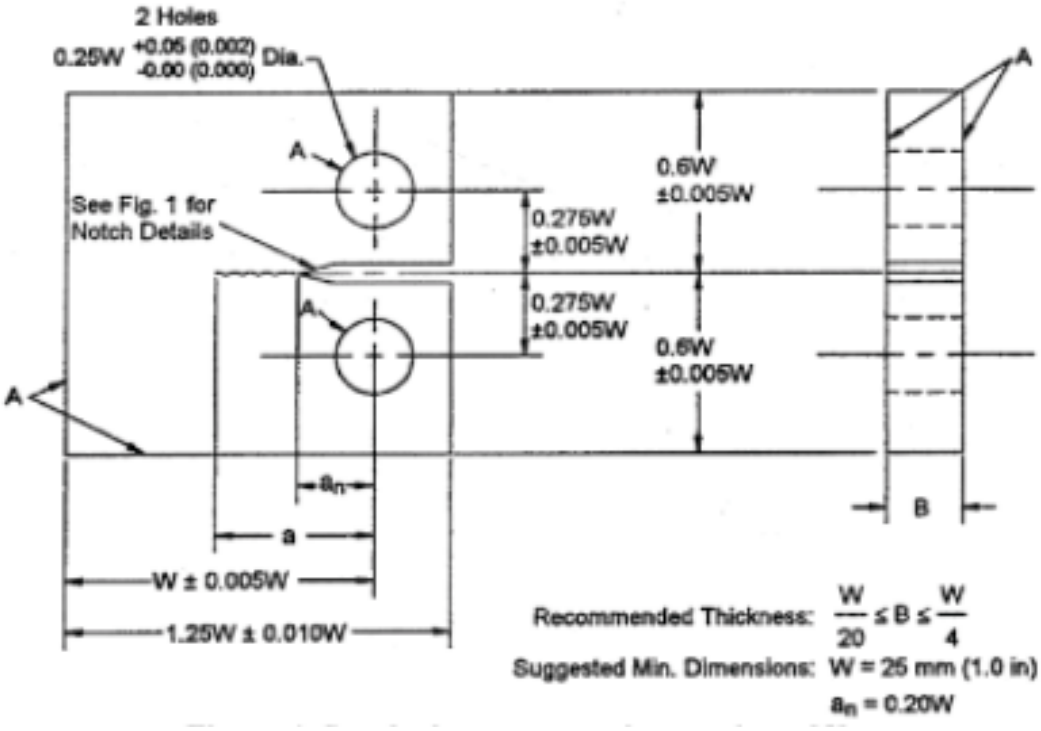

Figure 1: Example CT Notch Specimen [5]

The implemented system would use the electrical potential difference method to determine crack length. This is a measured, non-visual, method that relies on the differing electrical properties of the material as the crack is evolved through it. As the crack evolves the resistance will increase (due to a reduced surface area) and subsequently for any constant current the measured voltage across the sample will similarly increase. The specific potential difference method involved a reference sample which would never have any stress applied to it. By comparing the sample voltage against

the reference voltage at each measurement and applying specific equations, that will be evaluated later in the report, it is possible to determine the crack size of the sample. Figures 2 and 3, seen below, show a general circuit diagram for the samples and a diagram for the frame that the samples will be inserted into; together these two diagrams describe the majority of the system that needs to be controlled.

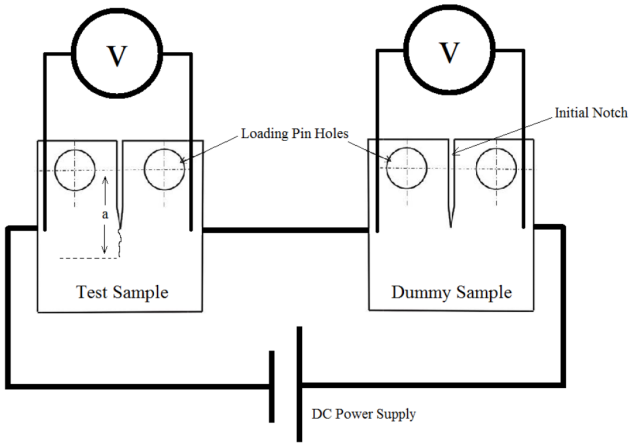

Figure 2: A circuit diagram of the sample connections.

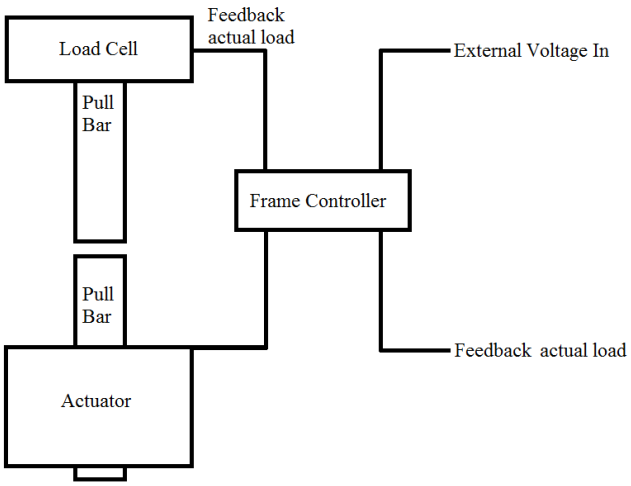

Figure 3: A diagram to show an overview of the frame design into which a sample would be placed.

The system outlined above does include some potential shortfalls. It is possible that if there is a temperature change the electric properties of the material will vary greatly, this causes the calculation of crack length to similarly change. In order to counteract this effect it it important to constantly measure and adjust the temperature if necessary using proportional-integral-derivative aided control. It is highly unlikely, but still possible, to get shorting across the crack. However, most materials develop an oxide layer soon after the crack is formed thereby reducing the probability that this will occur.

When conducting any FCGR test an important facet to account for is the gradient of the stress intensity factor K, which is a function of force P, crack size a and the specific geometry previously mentioned. The normalised gradient of K, which is defined as "the fractional rate of change of K with increasing crack size' [1] is given by the following equation:

$$C = \frac{1}{K} \cdot \frac{dK}{da} = \frac{1}{\Delta K} \cdot \frac{d\Delta K}{da} \tag{1}$$

This equation leads to the following three options for the normalised K-gradient:

1. **Increasing** K - In this scenario C is always positive. To achieve this the maximum value of K (also known as K_{max} is constantly increasing. As K is the stress intensity factor this test needs to maintain a constant load applied to the sample. This is because as the crack grows the value of K also grows, due to the decreasing material integrity. Increasing K tests are generally used for materials where the rate of crack growth with respect to each cycle $\frac{da}{dN} > 10^{-8}m$.[3]

2. **Constant** K - In this scenario C is always exactly, or approximately, zero. For this test the change in ΔK should be constant with the change in crack size. As such, as the number of cycles increases the system must begin shedding load at a rate equal the the amount that the stress intensity factor would usually be increasing. This involves predicting the rate of change of ΔK through the use of a computer automated test control procedure. As this is not technically a stand-alone option but rather an extension of the decreasing K method it is not mentioned in either the American or British test standards.[3]

3. **Decreasing** K - In this scenario C is always negative. In order to achieve this result K_{max} is gradually decreased as cycle number N increases. This means, similarly to constant K that the system needs to shed the applied load, this can be done gradually or incrementally. Regardless of the method applied it is important to ensure $C > -0.1mm^{-1}$ (for the general case, specific values vary dependant upon geometry and material). The equation applied to keep the value of C approximately constant is given below:

   $$\Delta K_{i(j)} = \Delta K_{i(j-1)} e^{C\Delta a_{(j-1)}} \tag{2}$$

   Where $\Delta K_{i(j)}$ and $\Delta K_{i(j-1)}$ are the initial stress-intensity factor range at step j and $j-1$ respectively and $\Delta a_{(j-1)} = [a_{(j)} - a_{(j-1)}]$ is the crack extension at the preceding constant force range $\Delta F_{(j-1)}$. As such, by predicting crack size a is is possible to predict the desired ΔK value. This method is used for materials with $\frac{da}{dN} < 10^{-8}m$. [3]

These three are the three tests that would need to be performed on any given specimen in the system.

2.2 The Fatigue Process

As previously stated in FCGR testing the crack propagation is measured as a function of the stress intensity factor. For such testing there are three main stages shown in Figure 4 below:
From Figure 4 it can be observed that there is a threshold value of ΔK below which fatigue cracks will not propagate (Stage I). The second region, and the one that is important for FCGR testing, has a linear relationship between $log\left(\frac{da}{dN}\right)$ and ΔK. The third region shows material failure due to K_{max} approaching the fracture toughness. For the purposes of the project both regions I and III do not need to be evaluated as they rely on microstructure and flow properties.

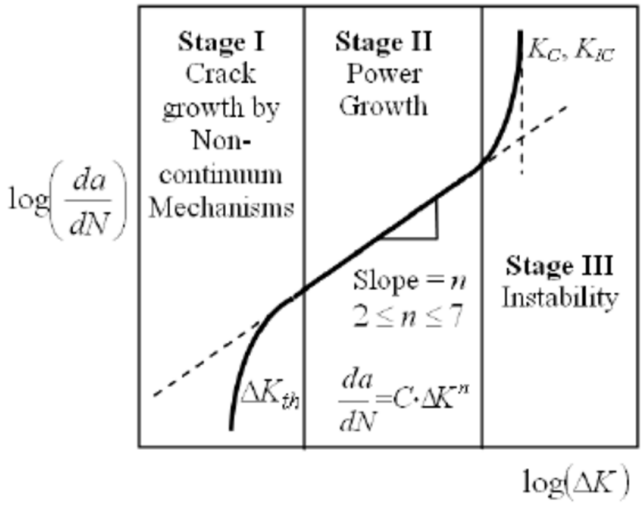

Figure 4: The three stages of crack propagation as a function of stress intensity factor. [8]

2.2.1 Crack Propagation Laws

From the visual above it is possible to determine that the crack growth rate must be expressed in terms of the stress intensity range ΔK, the stress intensity ratio $R = \frac{K_{min}}{K_{max}}$ and H the stress history. This leads to the equation:

$$\frac{da}{dN} = f(\Delta K, R, H) \tag{3}$$

This leads us to the most generally accurate and therefore popular function to determine of these factors is Paris' law. This suggests, where C and m are material constants, that:

$$\frac{da}{dN} = C\Delta K^m \tag{4}$$

The material constants in this (and similar) equations are the aims of the system to be developed. This equation allows for the prediction, assuming that Y the material factor is independent of a, of the number of cycles before material failure through the derivation shown below:

$$\begin{aligned} K &= \sigma Y\sqrt{a\pi} \\ \Delta K &= \Delta\sigma Y\sqrt{a\pi} \\ \frac{da}{dN} &= C\left(\Delta\sigma Y\sqrt{a\pi}\right)^m \\ \int_0^{N_f} dN = \int_{a_i}^{a_c} \frac{da}{C(\Delta\sigma Y\sqrt{a\pi})^m} &= \frac{1}{C(\Delta\sigma Y\sqrt{a\pi}} \int_{a_i}^{a_c} a^{-\frac{m}{2}}\, da \\ N_f &= \frac{2\left(a_c^{\frac{2-m}{2}} - a_i^{\frac{2-m}{2}}\right)}{(2-m)C(\Delta\sigma Y\sqrt{a\pi})^m} \end{aligned} \tag{5}$$

Where σ is the uniform tensile stress, a is the crack length, i is any initial value, f is any final value, and Y is a material factor[9]. The number of cycles before material failure is an important facet in any industry where material fatigue is a factor. There are, however, a few inconsistencies in Paris' law, it does not account for R or H as previously stated and it is only applicable for uniaxial and long cracked loading (ie. it must be in region II to be applicable).

2.3 Crack Size Calculation

The specific calculation of the crack size a is dependant upon the geometry of the specimen. For all of these methods detailed below the error (for measurements in the range used by the system) should be no worse than 0.1% with some highly conductive materials lowering the error to below 0.01%; this error, of course, can vary dependant upon geometry, material and instrumentation. The total list of geometries that the final product could acomodate were:

- Compact Tension - C(T)
- Middle Tension - M(T)
- Eccentrically-loaded Side Edge Tension - ESE(T)
- Corner Crack Tension - CC(T)
- Single Edge Notch - SEN B3, SEN B4, SEN B8
- Single Edge Notch Tension - SEN(T) Clamped, SEN(T) Pinned

Each of these geometries must be handled separately. However, only three of the geometries have specific equations for the crack size calculation with the rest all working off a pre-determined polynomial curve.

2.3.1 C(T) geometry

The C(T) geometry has an expression for the crack size given by:

$$\frac{a}{W} = B_0 + B_1\left(\frac{V}{V_r}\right) + B_2\left(\frac{V}{V_r}\right)^2 + B_3\left(\frac{V}{V_r}\right)^3 \tag{6}$$

In this equation a is the crack size, W is the sample width, V is the current voltage, and V_r is the reference voltage determined either by the dummy or by taking the first value of voltage. Any B value is a constant given by: $B_0 = -0.5051$; $B_1 = 0.8857$; $B_2 = -0.1398$ and $B_3 = 0.0002398$. This expression was developed by Hicks and Pickard through finite element analysis techniques before being verified through analogue and experimental techniques. This equation works for the range $0.24 < \frac{a}{W} < 0.7$ this range is implemented as a failsafe termination condition of the system in order to ensure accurate testing. ([6],[1])

2.3.2 M(T) Geometry

The M(T) geometry derives it's crack size calculation from the work of H.H. Johnson, who's 1965 paper analytically derived the 'Johnson's equation' by assuming an infinitely long specimen [1]. This assumption means that the relationship stated below is only valid for cases in which the current density is uniform at a cross section remote from the crack plane, it also requires that the voltage is measured on the centre line of the specimen across the crack plane. It should also be

noted that, as mentioned above, the DC current method is susceptible to thermoelectric effects. Johnson's equation is given by:

$$a = \frac{W}{\pi} \cos^{-1} \left[\frac{\cosh\left(\frac{\pi}{W} Y_0\right)}{\cosh\left[\frac{V}{V_r} \cosh^{-1}\left[\frac{\cosh\left(\frac{\pi}{W} Y_0\right)}{\cos\left(\frac{\pi}{W} a_r\right)}\right]\right]} \right] \tag{7}$$

For the M(T) geometry the variables are defined as such: a is the crack size; a_r is a reference crack size from another method (the system uses the previously calculated value); W is the specimen width; V is the measured potential difference; V_r is the measured voltage corresponding to a_r and Y_0 is the voltage measurement lead spacing from the crack plane. For the M(T) geometry the following condition must be met $0 < \frac{a}{W} < 0.5$ else the equations for both crack size as well as stress intensity factor K become inaccurate.[7]

2.3.3 ESE(T)

The ESE(T) geometry also uses the Johnson equation 7 to calculate crack size. However, due to the technical aspects of this geometry it should be noted that the 'width' that is used to calculate the crack size is actually defined as $\frac{W}{2}$ and as such must be treated differently from the M(T) sample.

2.3.4 All other geographies

All other geographies cannot, to a reasonable degree of accuracy for all materials, be evaluated analytically at this time. Due to this, each sample must have an identical sample tested upon using a different method. These values are then used to create a polynomial curve within the range of the measured values.This can be done through regression parameters given by the least squares method as applied to a second-order polynomial curve or using more complex methods to produce higher order polynomial curves and simply reading the related crack size for any voltage from the curve.

2.4 Stress Intensity Factor Calculation

The stress intensity factor K also has different calculations dependant upon the sample geometry. It does, however, also have a generalised equation for some standard geometries given by:

$$K = \frac{F}{BW^{\frac{1}{2}}} g\left(\frac{a}{w}\right) \tag{8}$$

Where the stress intensity factor geometry function, $g\left(\frac{a}{W}\right)$ for each standard specimen configurations is calculated dependant on the geometry. Examples of $g\left(\frac{a}{w}\right)$ can be found in the appendix. The two exceptions to this generalised rule are shown below, all the equations have been developed through both algebraic as well as experimental means. [3]

2.4.1 M(T)

$$\Delta K = \frac{\Delta P}{B} \sqrt{\frac{\pi\alpha}{2W} \sec\left(\frac{\pi\alpha}{2}\right)} \tag{9}$$

2.4.2 ESE(T)

$$\begin{aligned} \Delta K &= \left[\frac{\Delta P}{(B\sqrt{W})}\right] F \\ F &= \alpha^{\frac{1}{2}}[1.4+\alpha][1-\alpha]^{-\frac{3}{2}} G \\ G &= 3.91 - 10.88\alpha + 26.25\alpha^2 - 38.9\alpha^3 + 30.15\alpha^4 - 9.27\alpha^5 \\ \alpha &= \frac{a}{W} \end{aligned} \tag{10}$$

2.5 Data Reduction Techniques

Polynomial regression methods are integrated into the system to ensure all values used in calculations are as accurate as possible, and as a method of calculating the rate of change of crack size with cycle number $\frac{da}{dN}$. There are two distinct methods of polynomial regression. A first-order polynomial referred to as the 'Secant' method and the second-order polynomial for sets of $2n+1$ successive data points where n is usually 1,2,3 or 4. The secant method is formally defined by equation 11:

$$\frac{da}{dN}_{\overline{a}} = \frac{(a_{i+1} - a_i)}{(N_{i+1} - N_i} \tag{11}$$

As $\frac{da}{dN}$ is the computed average rate, the average crack size $\overline{a} = \frac{1}{2}(a_{i+1} + a_i)$ is used for calculations of ΔK. The polynomial method is shown in equation 12:

$$a_i = b_0 + b_1\left(\frac{N_i - C_1}{C_2}\right) + b_2\left(\frac{N_i - C_1}{C_2}\right)^2 \tag{12}$$

For this equation, a_i is the fitted crack size of datapoint N_i, b_0, b_1, b_2 are regression parameters given by the least squares method, $C_1 = \frac{1}{2}(N_{i-n} + N_{i+n})$ and $C_2 = \frac{1}{2}(N_{i+n} - N_{i-n})$.[1]

3 Project Management

This section covers the project management for the development of the FCGR system, including management structure and the Gantt chart. In terms of general project management a form of agile project management was implemented where, members of the team could work on whichever next task needed completing based on the priority of the task and individual strengths of the team member.

3.1 Management Structure

As part of the initial briefing weeks a decision had to be made about, based on individual strengths, a management structure for our group. This included designating areas of work for administrative tasks such as contacting Exova and filling out risk assessments. As a group the following structure was decided.

Dominic Reeves	Team Leader	-Overseeing everyone's progress on tasks to ensure milestones and deliverables are met. -Designates tasks if necessary.
Colette	Administration and Communications Officer	-Sets Meeting agendas -Takes minutes in meetings. -Communicates with the company contact, prints out all communications to the rest of the group.
Jacob	Technician	-Completes all tasks in a timely manner. -Focus on software element of the project.
Michael	Technician	-Completes all tasks in a timely manner. -Focus on hardware element of the project. -Fills out and updates Risk Assessment forms.

3.2 Project Timeline - Gantt Chart

The Gantt Chart is figure 18 and can be found in the appendix. The intention was to focus on the analysis classes first to ensure that they all worked individually from the rest of the system, implementing the equations described above before focusing on the communication between hardware and the control aspect of the system, this was to ensure that the more basic parts of the system were fully functional before expanding it to encompass the other aspects. These areas were revisited later on in the project for further testing but, apart from that, were not changed again except to connect them to all the other classes. How well the project kept to the Gantt chart will be evaluated in further detail later in the report but it should be mentioned that the time required for all tasks in work package 2 were underestimated and work package 4 was never implemented due to changes in the system design. The only other task that could not be implemented was 8.2 which could not be done due to availability of the engineering department test frames.

4 Design

4.1 Software Design

The software requirements of the system, outlined in section 1.1, can effectively be split into two components. The first components was the processing of data, this included the data storage, failsafe implementation, analysis methods and live access of the data. The second component was the hardware control which comprised, in itself, of two further components, the inputs and outputs of the system. In terms of outputs the system had to provide the correct current to the sample and correct wave function to the frame controller. In terms of inputs, the system had to take voltage readings from the sample as well as the frame for comparison purposes. An important facet of the decision making process was how these two components would be combined and how data would be transferred between them.

4.1.1 Initial Design

This section will discuss the initial prediction for how the system would work from a software perspective, detailing in rough the general flow of the program and giving some idea of the methods that would need to be implemented.

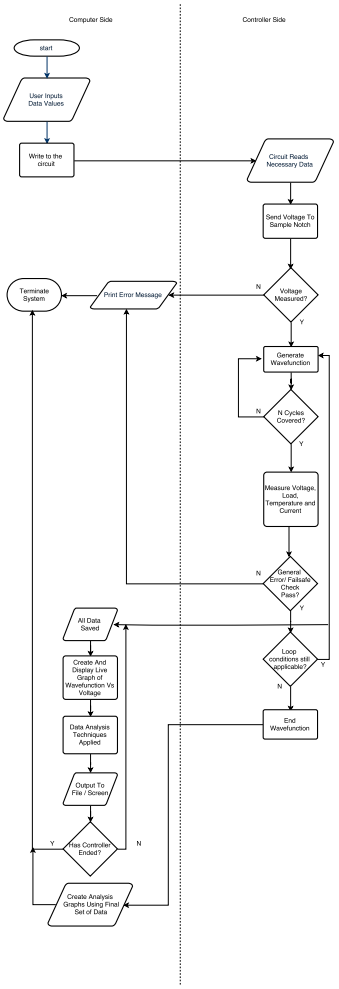

Figure 5: The initial software flowchart.

Figure 5 shows the first rough design for the software flowchart. The initial form involved using a single board processor as a main controller for all hardware related control while the computer focused on the analysis component of the overall design. The user would input the necessary values on the computer side of the application, this would then be sent to the external processor which would take the necessary inputs and use them to communicate with the necessary hardware components before sending back the results. This setup was decided upon in order to stick better to the 'all-in-one' aspect of the brief, by having the control as part of an all in one hardware system with the computer side simply analysing data. It was also hoped that, because two separate systems were doing the controlling and analysing, the efficiency of the system would be increased as each individual system would have to do less calculations per cycle. The use of the external processor simplified the decision making process when it came to how to combine the two different components of the software as, using this method, they didn't need to be combined at all; the external processor would simply pass the necessary data back through to the main computer to be analysed. The main potential problems were the exact specifics of how to control the hardware, and how the external processor would be controlled in terms of it's command to start and stop, past that both systems would work independently of each other. It was also mentioned that it may be beneficial to include a proportional-integral-derivative controller (PID) to the system, this was originally going to be an additional hardware component but, upon further investigation, it was determined that implementing the code into the controller itself in order to better control the weighting of each of the proportional, integral and derivative components. A PID controller is 'A feedback controller designed to generate an output that causes some corrective effort to be applied to a process so as to drive a measurable process variable towards a desired value'. They are incredibly important for ensuring output values from the hardware match the requested software values. [11]

4.1.2 Final Design

Through the development process a number of changes were made to the initial design. The first derivation from the plan was the two controller system, as the hardware components were determined it became evident that the any one board processor, unless it was running a windows operating system, was going to be incompatible with certain major pieces of hardware (such as the current and waveform generators) as the hardware provided was specifically designed for windows. On top of this it was found that the temperature probes, which were intended to work independently of the main system and simply take constant reading for the user to observe, could not operate outside of their inbuilt software and therefore no longer needed to be implemented into the system. The final system was run from a windows PC (as each of Exova Lancaster's frames has a PC attached to it regardless) and combined the two separate components without issue. The two components could be combined without efficiency loss as the analysis requirements only asked for a new data reading every half second, which happened to be more than ample time.

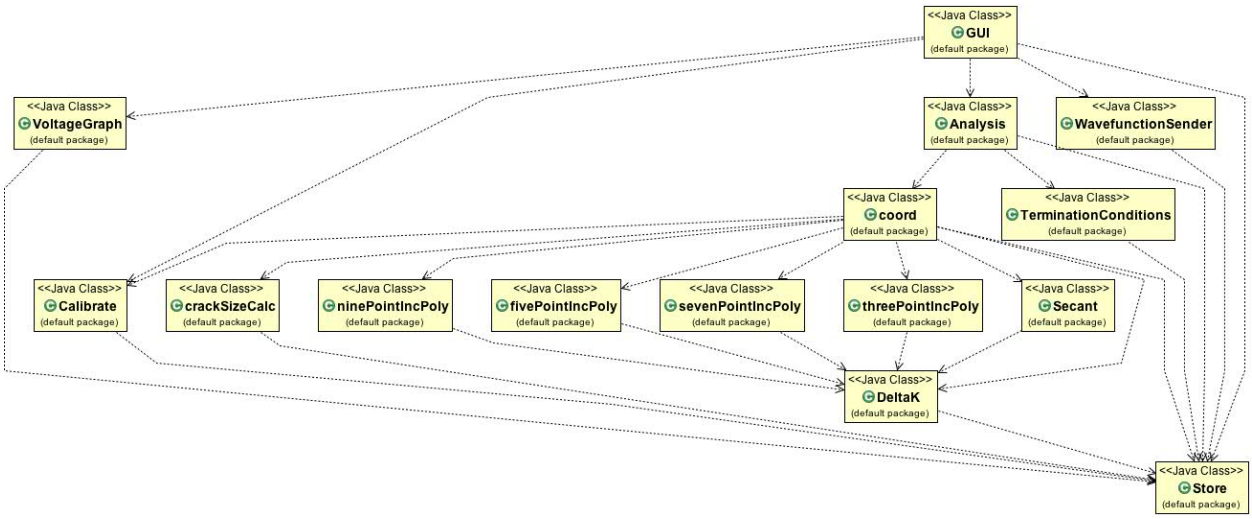

Figure 6: The final class diagram.

Unfortunately, due to hardware-software incompatibility, some of the additional functionality could not be implemented. The most important functionality missing in the final system was the ability to get a return voltage reading from the frame. This was due, despite the hardware manual claiming java compatibility, to the fact that the hardware required a .net framework to control. As the return voltage from the frame is not a vital part of the analysis system and is merely to ensure that all the hardware is working it was decided, both by the company and the team, that this additional functionality was not worth the licensing cost of a '.net bridge' software package to allow java to communicate with the system. When the current system was examined in more detail it was found that the frame controller already had a PID controller implemented. This meant that not only was a PID un-necessary but it actually would have been detrimental as multiple separate PID controllers acting on the same data interfere with each other and have a reduced efficiency than simply having one. A quick description of the role of each class can be found below:

- **GUI:** This is the main class for the system, it creates the Graphical User Interface (GUI) and, on a button click, ensures the correct datatypes have been entered before storing them as permanent values in the 'store' class. Once it has sent the values to the store it begins the calibrate class in order to generate a crack size polynomial (if necessary), begins the WaveFunctionSender class, sends the correct current to the current generator (as this is never to be changed it was un-necessary create a class dedicated to this) and finally begins the analysis class. It also allowed the 'Voltage Graph' button to be pushed, which executed the VoltageGraph class.

- **VoltageGraph:** This class, theoretically, would display the voltage values of wave function generator output and frame voltage with respect to time allowing the user to visually compare the two values and ensure the transfer was working correctly. Unfortunately, due to the software-hardware compatibility issue stated above, this was not an option for the final system and, as such, it simply displayed a current live graph of the dummy and live sample voltages.

- **WaveFunctionSender:** This class initialises the WaveFunctionGenerator, sending the

user designated wave function type, frequency and amplitude to the generator. It also has a method included that can change any of these values. However, due to the complexity of any other specimen par ΔK increasing (to the degree of accuracy that Exova would want) and the fact that they are not disclosed to reveal the specific equations that the third party currently implements, the system as it stands can only handle ΔK increasing and as such the wave function never needs to be changed.

- **Analysis:** The analysis class creates a graph frame with drop down menus of which analysis methods are to be implemented. It catches the voltage reading from the sample and dummy sample before sending them, along with values of cycle number, crack size, $\frac{da}{dN}$, and ΔK (which are calculated by calling to other classes using the user determined methods). The class proceeds to determine the values for the x and y axis of the live graph and display them for the user. It continues this cycle until one of the termination conditions is met.

- **Termination Conditions:** This class sorts through which method the user wants implemented, including any specific termination conditions and returns a boolean flag if any of the termination conditions have been met.

- **Coord:** The coord class calculates the user determined value for the data point to be printed to the live graph. It is mainly used as a sorting class, using the user choice and calling the relevant classes necessary to analyse the collected data.

- **Calibrate:** The most basic of the analysis classes. This class is initialised on the button press in GUI, it reads data points from a user created .csv file and fits a polynomial curve of user defined order to these points. It can then be called at any time, with a given voltage reading and will provide the corresponding crack size value on the polynomial curve that was created.

- **crackSizeCalc:** This class implements the necessary methods to calculate crack size for any specimen that doesn't simply require a polynomial curve fit, details of which are found in section **??**.

- **[...]IncPoly & Secant Classes** All these classes (three, five, seven, nine)IncPoly and Secant are all just implementations of the data set modification techniques outlined in the above sections, simply taking the data and determining a weighted average of the data points.

- **DeltaK:** This class takes the specimen type and calculates, using the relevant equations, the ΔK value for any given crack size utilising values specific to the crack from the store.

- **Store:** This is the main store of the program, holding all the variables required by the other classes to be accessed for analysis calculations. A store was used in leu of public variables to reduce complexity and because the values needed to be frequently updated and accessed and, during the development process, this helped reduce memory location related issues.

4.2 Hardware

Looking at the brief in section 1.1 it is possible to see that the hardware section of the project is split into a few major components. The first of which is the production of the wave function to the test frame, this needed to produce a voltage of $\pm 10V$ and any of the waveforms listed in the brief. It also needed to provide a constant current across both the dummy and test samples for the voltage drop testing method; for some of the specimens provided this would have to provide up to $50V$ and $10A$. Finally, the system would need a way of measuring the potential difference across the two samples that could be logged by the computer. Less vital components of the system were thermocouples to measure the temperature and ensure it was constant as well as an analogue to digital convertor to get voltage return from the frame, in order to ensure the output voltage was correct.

4.2.1 Initial

The initial design involved a one board processor, this would control all other hardware and reduce the number of direct connections to the computer. The first hardware task was to simply procure the necessary hardware components. The specific hardware components acquired were as follows:

Hardware Component	Role	Provided By
QPX 1200 Current Generator	Current generator for samples	Exova
TG5011 Wave-function Generator	Wave-function generator to the test frame	Exova
DataQ 145 Digital to Analogue Convertor	Digital to Analogue convertor for voltage response from frame	Exova
R-type thermocouples and amplifier	To measure the temperature of the samples and ensure it was kept approximately constant	Exova
Fluke 8808A digital multimeters	To measure the voltage over the test and reference sample	Lancaster University Physics Department Storage
Raspberry-Pi	To be used as the single board processor controller	Project Budget and Amazon.co.uk

The system would work as described in section 4.1, the single board processor would control and collect all the relevant data from the hardware before sending it back to the computer in the form of a .csv file. This sequence would occur by the controller initialising the wave function and current generators. It would then begin to record data from the digital multimeters (DMMs), the two thermocouples connected to the amplifier as well as the test frame through the digital-to-analogue convertor. The control would put the data through any necessary safety checks and analyse any errors where it could through the use of the PID controller (as mentioned in the software section, this was initially a separate piece of hardware but was eventually integrated into the software). The controller would then send off the data to the computer for analysis. Figure 7 below shows the initial schematic for the hardware including the connections between each component.

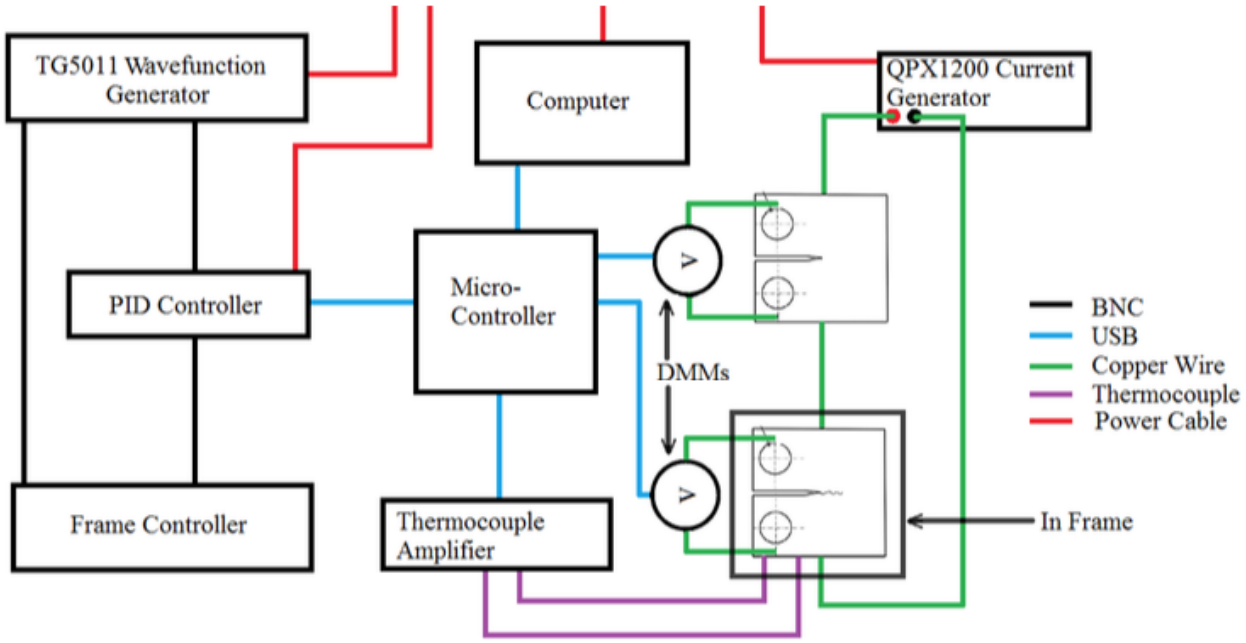

Figure 7: The initial design of the hardware. This diagram does not show the connection between the controller and the wave function generator although in reality they were connected via USB cables. This was due to uncertainty as to how a PID hardware device would work.

It is worth noting at this point that, in the initial design, there was a fair amount of confusion between which of the generators was the wave function generator and which was the current generator. This was due to the fact that the QPX1200 could not reach some of the measurements asked for in the briefing whereas the TG5011 could reach those values. As such there was an intermediate stage in the project where code was written and cabling was altered to account for these changes. This was quickly resolved by asking Exovas' industrial contact and the overall effect of this effect on the project timeline was negligible.

4.2.2 Final Design

The main change in the hardware was the removal of the Raspberry-Pi as a central controller. Even so, this was not a large change as every component was connected via USB cable regardless. The transfer between the old system and the new was a simple case of purchasing a USB hub to account for the lack of suitable sockets on the computer. Due to the hardware-software compatibility issues explained in section 4.1.2 the final design did not involve a connection back from the frame nor any temperature probes. The PID was removed, as explained, due to the potential interference between it and the frame PID controller. Apart from this there were no complications in the hardware component of the project. The final hardware design can be seen in figure 8.

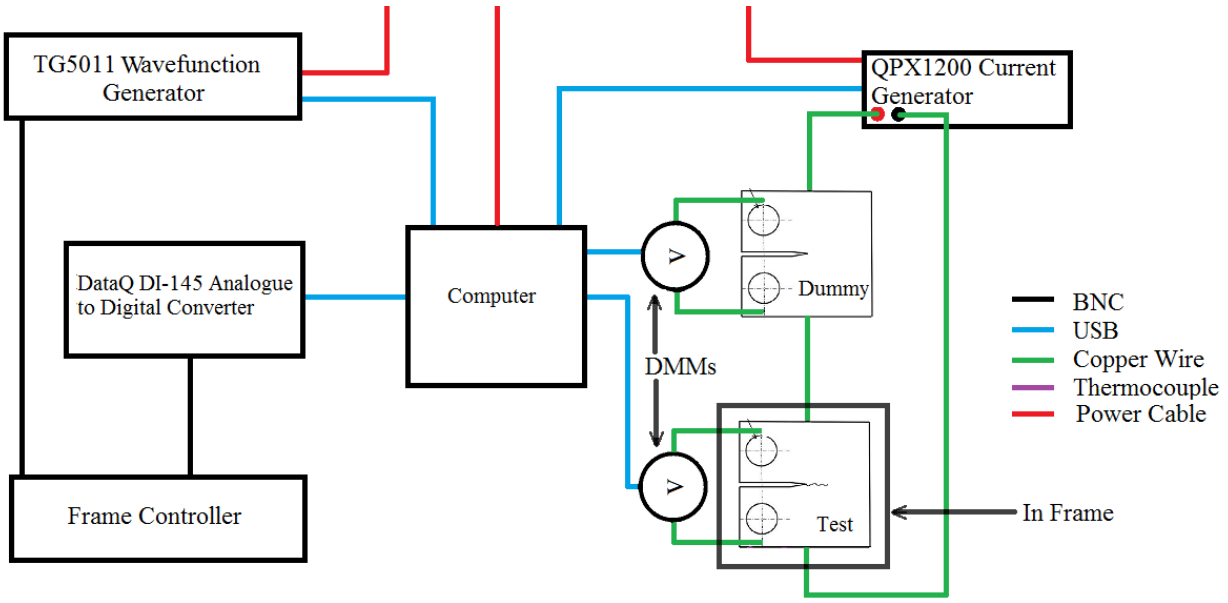

Figure 8: The final hardware design. This version includes the DataQ digital-to-analogue convertor as, had there not been compatibility issues, this is the ideal final design of the system.

5 Test Analysis

This section will evaluate the testing methods applied to the prototype as well as providing evidence to support the fact that the system works as intended. There were two testing methods implemented, other than the usual step by step testing that ran alongside the system development. The first was to hook up the prototype to a sample outside of the frame, this enabled the measurement of all the values compared to known sample values. More importantly this meant that the systems hardware connections were thoroughly tested and would output the correct values when asked. The sample was not put under fatigue strain because it would require full attachment to a frame followed by, to get any meaningful results, a testing time period longer than we could observe the system for. Provided that we could measure the output from the wave function generator the system could be tested to the same extent without strain this allowed us to collect the necessary data without incurring any fiscal loss or waste of time for Exova. The second method was the comparative analysis of pre-recorded data from a full sample test, by running the data through isolated analysis methods it was then possible to directly compare the effectiveness of these classes against the methods currently in use and, as such, analytically determine potential error in each one.

5.1 Live Sample Analysis

The following section will simply show graphs of the crack size, ΔK and $\frac{da}{dN}$ measurements from the live sample. It should be noted that the actual values displayed have little to no analytical meaning behind them, this is simply to show that the system works as intended with a hardware output that stays roughly constant. It should be noted that a few points of erroneous data have been removed from the sample, this is because they were approximately seven orders of magnitude larger than any other value. These anomalous results, including most of the fluctuation still visible in the graphs, can be explained by simply pointing out that the average voltage through the test sample was $3.2E-4$ and through the reference sample was $2.1E-4$. Such low voltage readings (when compared to the typical values $\pm 10V$) mean that any slight variation in the voltage measurement will result in large variance in the calculated values.

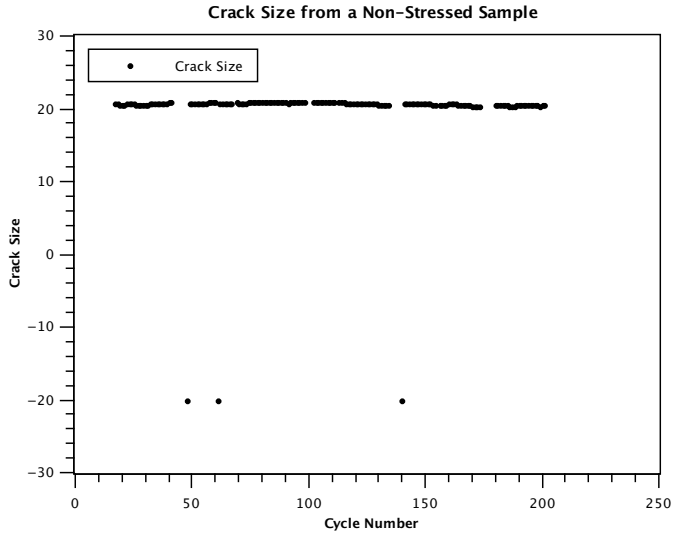

Figure 9: The approximately constant value of $\approx$ 20mm is an acceptable distance from the actual value of 23mm. Although this is a large difference numerically, when the test was initially ran the given values to the system of crack size was 20mm for both test and reference sample. Using this information the fact that the measurement hasn't changed when no stress has been applied is correct. If the correct values had been input initially the measurement output would be closer to the given value.

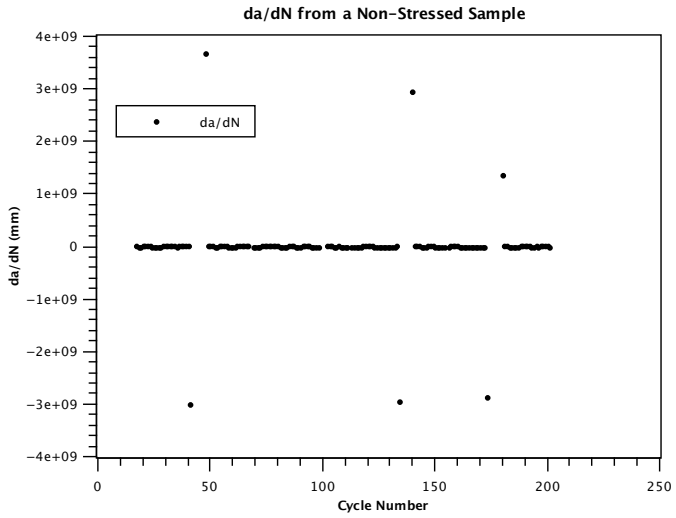

Figure 10: This graph shows $\frac{da}{dN}$ from the live data, an important facet to observe is that it contains exactly double the number of anomalous fluctuations as the crack size graph, this is due to the fact that for every anomalous crack size result there was also an equalising value in the $\frac{da}{dN}$. The fluctuations in this graph are extremely large, this is to be expected due to the fact that fluctuations in crack size were generally single blips meaning any change had to happen over a single cycle.

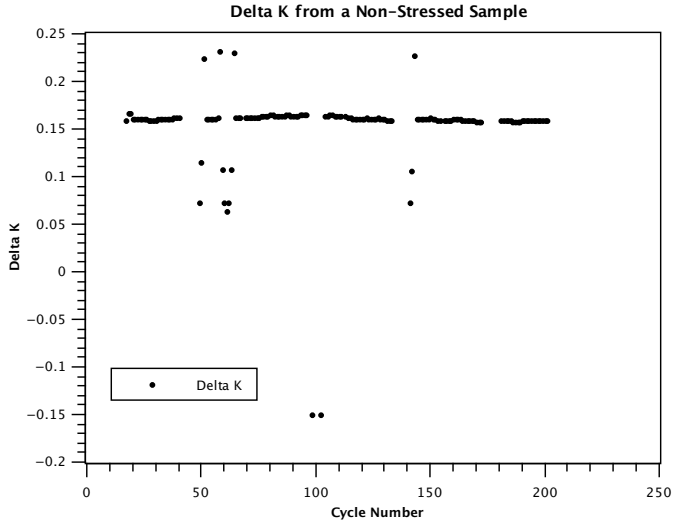

Figure 11: This graph includes a lot more fluctuation than either of the previous two. It is, however, much closer to it's actual value of zero when compared to typical values of ΔK as they are generally measured in $MPa\sqrt{m}$ whereas this is relatively close to zero.

5.2 Comparative Analysis

5.2.1 Crack Size Calculation

The raw data from the provided sample was ran through the crack size class (with slight modification so that the class could run independently of the rest of the system and instead take in data from a .csv file). The methods employed were designed in accordance with the equations outlined in section 2.3. The results of this data analysis are shown in figure 12.

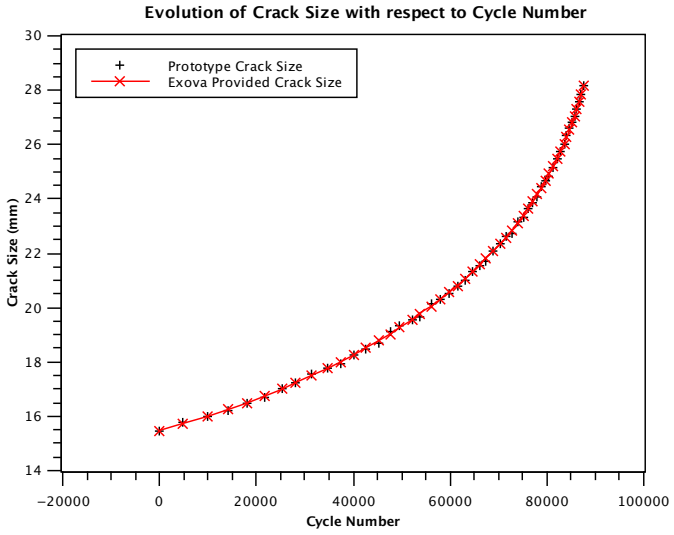

Figure 12: A comparative graph of crack size against cycle number. This evolution with time does not provide any important analytical information in terms of overall fatigue testing but instead is included as a visual representation of any error present.

Figure 12 shows a high level of correlation between the two sets of results with a maximum error between the two sets of $0.14mm$ corresponding to a 0.01 fractional difference. This fractional difference is well within the standard allowed range of $\pm 2\%$. From this set of data it's possible to observe the expected trend for crack evolution, as the cycle number increases in an increasing K test it is expected that the crack size will exponentially increase.

5.2.2 Crack Size Seven-Point Regression

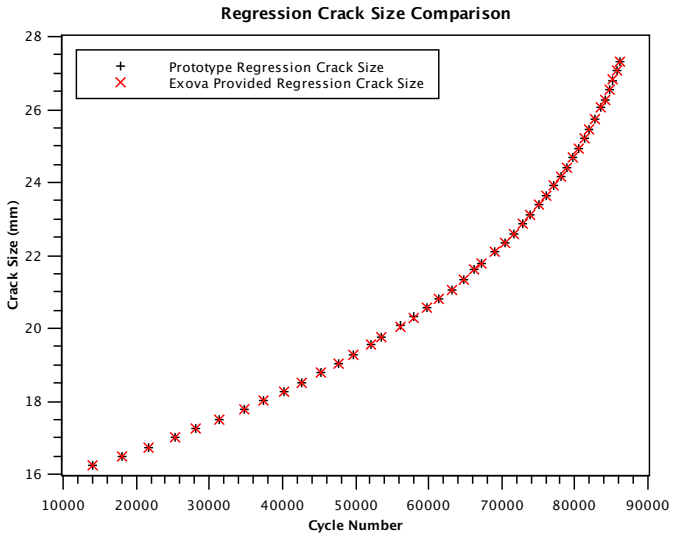

Figure 13: This graph shows the seven-point regressed data, as a result it has six less data points than the pure crack size calculation but with data points that much better match the pre-calculated values.

This graph simply shows the polynomial regression values of the graph in figure 12. The maximum difference between the values in this case, to two significant figures in order to match the given values, is 0.00 showing that the polynomial regression techniques improve the accuracy of the results and that the designed classes work as expected.

5.2.3 ΔK Calculation

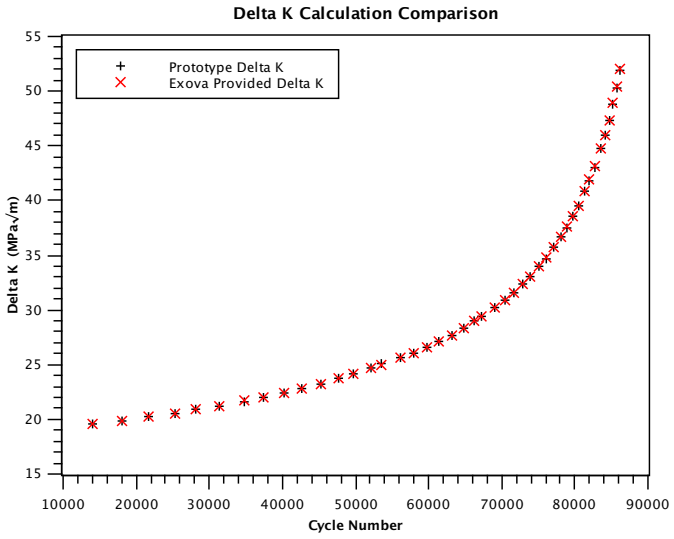

Figure 14: The provided and calculated values of Delta K based off previously calculated crack size values.

This graph was calculated with a modified DeltaK class, getting input values from a .csv file. Once again these values were compared against cycle number and, from the exponential increase in Delta K as crack size increases, it can be confirmed that an increasing K test was carried out. Comparing the system calculated values to those calculated by Exova's current system there was a maximum difference (error) of $0.13(MPa\sqrt{m})$ which corresponds to a fractional difference of 0.00 to the correct number of significant figures or a real value of 0.0025. Provided that the BSISO states an approximate error in this calculation of $\pm 4\%$ this set of data provides evidence towards the conclusion that the class was implemented correctly. Max difference = 0.13, 0.0025 fractional difference (0.00 to correct number of sig figs)

5.2.4 $\frac{da}{dN}$ Calculation

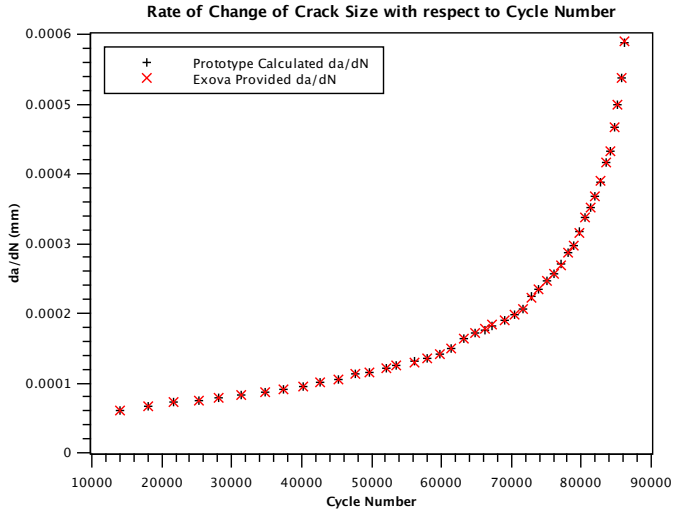

Figure 15: This graph shows the contrast between the calculated and provided data for the rate of change of crack size against the cycle number.

This calculation, based off the values from the polynomial regression method, and calculated in the same class, should and does have a very similar error to the crack size regression data points. The maximum difference of the calculated values when compared to the provided values is $0.00mm$, again this is only to the given number of significant figures as going any further than that would be imprecise. This reduction in error is an expected result of the polynomial method, with the higher the polynomial method the better error reduction for the data [10]. The figure 15 is in agreement with figures 12 and 13 as it shows that as the cycle number increases the rate of change of crack size similarly increases.

5.3 $\frac{da}{dN}$ against ΔK

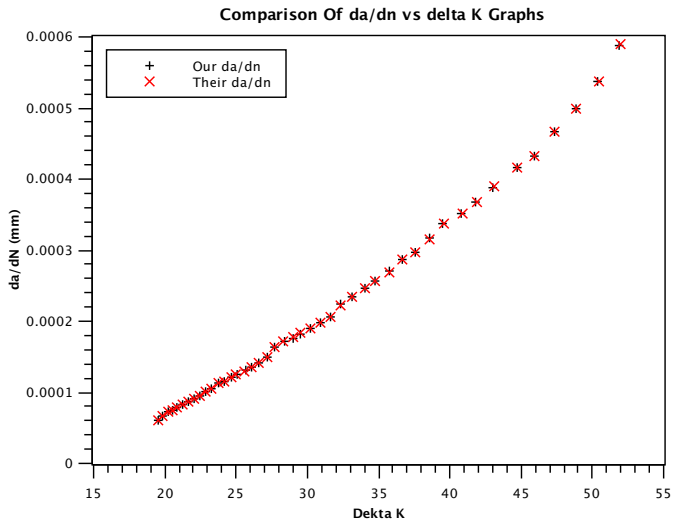

Figure 16: This graph plots the non-logarithmic graph of rate of change of crack size against ΔK to show that any compounded error is similarly small in accordance with the rest of the results.

Figure 16 shows a high level of agreement with the provided data, this is expected based off the accuracy of the previous graphs, it also shows the power law relationship explained in section 2.2 between $\frac{da}{dN}$ and ΔK values. This provides evidence to suggest that the sample was in the second stage, as is necessary for FCGR testing.

5.4 Paris' Law Evaluation

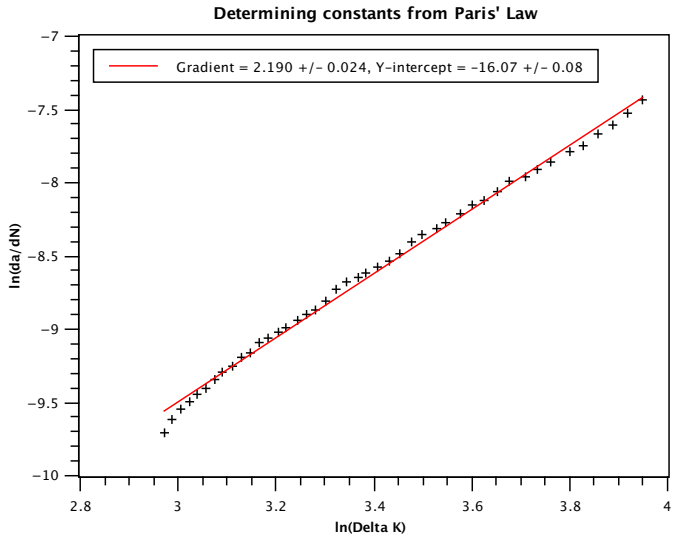

Figure 17: This graph shows, what is effectively, the second stage of fatigue crack growth rate testing shown in 2.2. This is observable due to the linear logarithmic relationship.

This is a non-comparative graph showing the Paris' Law relation for calculated values between the logarithmic rate of change of crack size and the logarithmic stress intensity factor. The fact that this produces a linear relationship again shows that the specimen was in the correct crack propagation stage. Applying the Paris' Law (equation 4) to this linear fit allows us to find values for the constants m and C for this specimen. The value of m is simply the intercept of the logarithmic graph, and as such has a value of $m = 2.190 \pm 0.024$. The value of C is given by $e^{y-intercept}$ and as such gives us a value of $C = (1.0544 \pm 0.0850)E - 7$ (using exact value and staying to the stated number of significant figures in provided data). When comparing these to the produced values of $m = 2.185$ and $C = 1.0683$ both of the calculated values fall within experimental range and have a fractional difference of 0.002 and 0.013 respectively. With all of the values falling within an acceptable range of error it is now possible to say that the system fulfils the full range of requested analytical techniques.

6 Conclusion

The design and implementation of the fatigue crack growth rate system met the vast majority of the company's control and analysis standards. Using Exova and Lancaster University provided hardware, the system could accurately control the fatigue frame and data collection from all hardware apart from the frame voltage response and thermocouples, two non-critical parts of the testing process. It could also not implement 'spectrum' wave functions as the hardware was not capable of implementing any wave functions that were not pre-programmed. The system was shown to record and analyse data with occasional fluctuation, however this was down to the low voltage applied across the sample and subsequent accuracy fluctuation from measurements in the digital multimeters. When examined quantitatively the analysis methods included in the system were found to diverge from given values by a minor amount. The largest fractional error of any quantity being 0.01 fractional difference in the crack size calculation before polynomial regression correction. The initial system design was overcomplicated, implementing hardware and software components that were un-necessarily, namely the inclusion of the Raspberry-Pi. Further work to be done on this project would be to create a non-prototype version of the software/hardware. To do this the code would be re-written in a .net language such as Visual Basic in order to implement the additional functionality requested, it would also be important to develop exact numerical methods to implement the constant and decreasing K methods, the basic outline of which has been explained in section . Once this new system was developed more in depth testing of each individual class as well as the system interaction with a frame as a whole would be required.

References

[1] Exova, Fatigue Crack Growth Rate Testing

[2] American Section of the International Association for Testing Materials *ASTM E647-15: Standard Test Method for Measurement of Fatigue Crack Growth Rates.* West Conshohocken, PA: ASTM International; 2015.

[3] British Standards Institute. *BS ISO 12108: Metallic materials Fatigue testing Fatigue crack growth method.* London: British Standards Institute; 2012.

[4] Suresh S., *Fatigue of materials. 1st ed.* Cambridge [u.a.]: Cambridge Univ. Pr.; 2006.

[5] Allen, D.J., *Creep Performance of Dissimilar P91 to Low Alloy Steel Weldments* London, Parsons, IOM, 2006.

[6] Hicks, M.A., and Pickard, A.C., *A comparison of Theoretical and Experimental Methods of Calibrating the Electrical Potential Drop Technique for Crack Length Determination* Int. Journal of Fracture, No. 20, 1982.

[7] Johnson, H.H. *Calibrating the Electric Potential Method for Studying Slow Crack Growth* Materials Research and Standards Vol 5, No. 9, Sept 1965.

[8] Lucian, M.T., and Claudiu, O.P., *STRESS INTENSITY FACTOS ANALYSIS ON THE CRACKS IN THE HERTZIAN STRESSES FIELD OF TEETH GEARS*, The 10th International Conference on Tribology, Bucharest, Romania, 2007.

[9] Paris, P., and Erdogan, F., *A Critical Analysis of Crack Propagation Laws.* Journal of Basic Engineering, 1963, pg 528 -532.

[10] Kysz, S., and Leski, A., *Applied Fracture Mechanics., Chapter: 7,* Publisher: INTECH, Editors: Belov A., 2012, pp.197-228

[11] htmladdnormallinkVance J. VanDoren, Familiar examples show how and why proportional-integral-derivative controllers behave the way they do., 2000http://www.controleng.com/single-article/understanding-pid-control/ebf9ab7fe3e5571f83901e0b8f3d8f07.html

7 Appendix

7.1 Stress Intensity Factor Geometry Functions

C(T)

$$g\left(\frac{a}{w}\right) = \frac{(2+\alpha)(0.886 + 4.64\alpha - 13.32\alpha^2 + 14.72\alpha^3 - 5.6\alpha^4)}{(1-\alpha)^{\frac{3}{2}}}; \alpha = \frac{a}{W} \tag{13}$$

CC(T)

$$g\left(\frac{a}{w}\right) = \left(\frac{\theta}{cos\theta}\right)^{\frac{1}{2}} (0.7071 - 0.0072\theta^2 + 0.007\theta^4); \theta = \frac{\pi a}{2W} \tag{14}$$

SEN B3

$$g\left(\frac{a}{w}\right) = \frac{6\alpha^{\frac{1}{2}}}{[(1+2\alpha)(1-\alpha)^{\frac{3}{2}}]}[1.99 - \alpha(1-\alpha)(2.15 - 3.93\alpha + 2.7\alpha^2]; \alpha = \frac{a}{W} \tag{15}$$

SEN B4 & SEN B8

$$g\left(\frac{a}{w}\right) = 3(2\tan\theta)^{\frac{1}{2}}\left[\frac{0.923 + 0.199(1-\sin\theta)^4}{\cos\theta}\right]; \theta = \frac{a\pi}{2W} \tag{16}$$

SENT Pinned Specimen

$$g\left(\frac{a}{w}\right) = \sqrt{2\tan\theta}\left[\frac{0.752 + 2.01\alpha + 0.37(1-\sin\theta)^3}{\cos\theta}\right]; \theta = \frac{\pi a}{2W} \tag{17}$$

Clamped Specimen

$$g\left(\frac{a}{w}\right) = (1-\alpha)^{\frac{-3}{2}}[1.9878\alpha^{\frac{1}{2}} \quad -2.9726\alpha^3 2 + 6.9503\alpha^{\frac{5}{2}} - 14.4476\alpha^{\frac{7}{2}} + 10.0548\alpha^{\frac{9}{2}} + ... \\ 3.4047\alpha^{\frac{11}{2}} - 8.7143\alpha^{\frac{13}{2}} + 3.7417\alpha^{\frac{15}{2}}] \tag{18}$$

$$\alpha = \frac{a}{W}$$

7.2 Gantt Chart

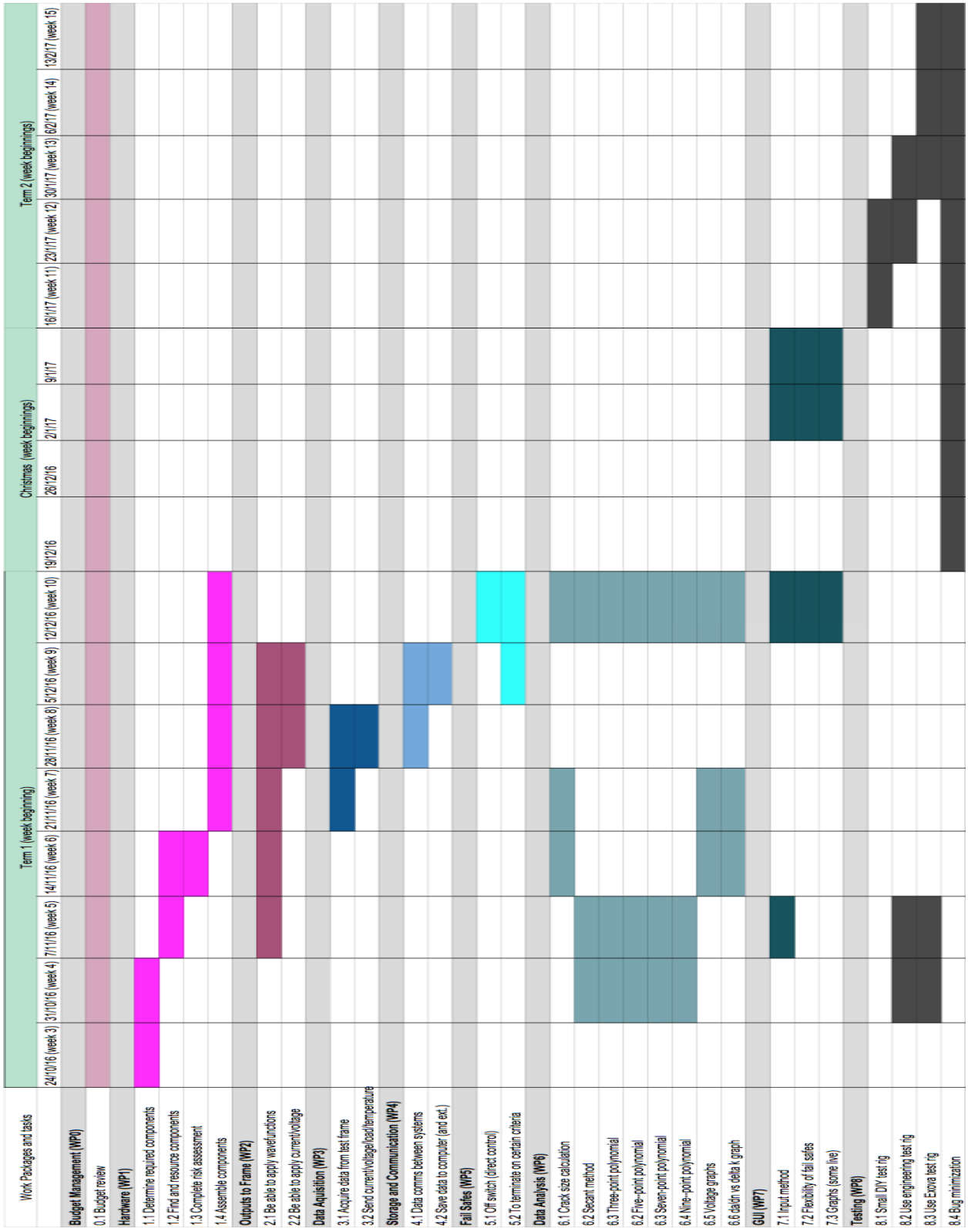

Figure 18: The initial Gantt Chart with predicted task times.